Table S1. Primary antibodies used in this study.

Source	Primary antibodies	Catalog no.
Abcam	Rabbit anti-p16^{INK4a}	ab108349
Abcam	Rabbit anti-p21	ab109199, ab109520
Abcam	Mouse anti-Vimentin	ab8978
Abcam	Rabbit anti-GATA4	ab227512
Abcam	Rabbit anti-ATG7	ab133528
Abcam	Mouse anti-EGFP[a]	ab184601
Santa Cruz Biotechnology	Mouse anti-p16^{INK4a}	sc-1661
Synaptic Systems	Rabbit anti-m6A	202003
Cell Signaling Technology	Rabbit anti-LC3B	43566
Proteintech	Rabbit anti-p62	18420-1-AP
Proteintech	Rabbit anti-METTL3	15073-1-AP
Proteintech	Rabbit anti-YTHDF1	17479-1-AP
Proteintech	Rabbit anti-YTHDF2	24744-1-AP
Proteintech	Rabbit anti-ACTB	20536-1-AP

Table S2. Information of the patients with total knee arthroplasty.

Patient Number	Gender	Age	Body-mass index (kg/m^2)	Kellgren-Lawrence grading scale
1	Male	51	22.64	4
2	Male	53	23.46	4
3	Female	53	20.85	3
4	Male	54	22.01	3
5	Male	58	23.25	4
6	Male	59	19.7	3
7	Female	60	23.76	4
8	Male	60	24.85	4
9	Female	61	24.13	3
10	Female	63	23.68	4

Table S3. Information of the patients with arthroscopic meniscus repair.

Patient Number	Gender	Age	Body-mass index (kg/m^2)	Kellgren-Lawrence grading scale
1	Male	51	21.33	0
2	Male	55	23.58	1
3	Female	55	22.49	0
4	Male	57	24.32	1
5	Male	57	22.57	0
6	Female	58	19.95	0
7	Male	56	21.37	0
8	Female	59	20.7	1
9	Male	60	23.27	0
10	Male	62	23.93	0

Table S4. Characters of patients.

	Non-OA (n=10)	OA (n=10)	P value
Age	57 ± 3.06	57.3 ± 4.10	0.90
Male:Female	7 : 3	6 : 4	0.64
Body-mass index	22.35 ± 1.46	22.83 ± 1.58	0.49
Kellgren-Lawrence	0.3 ± 0.48	3.6 ± 0.52	< 0.001

Data are presented as mean ± SD. Independent t test for continuous variables and chi-square for categorical values.

Table S5. Primers used for qPCR.

	Primer sequence (5'-3')	
Target gene	Forward	Reverse
Human IL1B	GAAATGATGGCTTATTACAGTGGC	AAAGATGAAGGGAAAGAAGGTGC
Human IL6	CCTTCGGTCCAGTTGCCTTCTCC	GCCAGTGCCTCTTTGCTGCTTTC
Human IL8	TTTCAGGAATTGAATGGGTTTGC	TGTGAGGTAAGATGGTGGCTAAT
Human IL13	CAGTGCCATCGAGAAGACCCAGAG	TCCCTAACCCTCCTTCCCGCCTA
Human MMP3	ACAAGGAGGCAGGCAAGACAGCA	GCCACGCACAGCAACAGTAGGAT
Human MMP13	GGTGACTGGCAAACTTGACGATA	GGACCATTTAAGAGTTCGAGGGA
Human CDKN2A	AGGGCTTCCTGGACACGCTGGTGGT	CGGCATCTATGCGGGCATGGTTA
Human CDKN1A	TGATTAGCAGCGGAACAAGGAGT	TGGAGAAACGGGAACCAGGACAC
Human ATG3	TGAAGCAAAGCGAGGACAGACAG	ATCTACCCATCCGCCATCACCAT
Human ATG4B	GAGCCCGTTTGGATACTGGGTAG	CTGTCGATGAATGCGTTGAGGAC
Human ATG4D	GCTGTACCGTGGGCTTCTATGCTG	TACCGCTCTGTGGCTGAGGAGGA
Human ATG5	TGGAGGCAACCTGACCAGAAACA	AATGATGGCAGTGGAGGAAAGCA
Human ATG7	AGGTCAAAGGACGAAGATAACAATT	GGTACGGTCACGGAAGCAAACAA
Human ATG10	GTTGTTGGGCTGAATCTACCTCT	GTAAACTCTTGGCATTCTTCGTG
Human ATG12	CACCCATTGCTCCTACTTGTTAC	ACTGCCCTCTACTGGACTATTTG
Human ATG13	GCTTTACCTTGGATAGTTGCGTATT	GAACCTGGGATTAGAGGGAGATG
Human ATG14	GCTGGTCAACATTCTGTCTCATA	GACTCCTCAAGGTCTGCTCGTAC
Human ATG16L1	CATTCCCGCTTCTGCTGGTTGCT	CCTCAGTTGCTCCGAGATGTGGC
Human METTL3	CGCAAGCTGCACTTCAGACGAAT	CACTGGAATCACCTCCGACACTC
Human METTL14	TCCCATGTACTTACAAGCCGATAT	ATTAGCAGTGATGCCAGTTTCTC
Human FTO	AGCACTGTGGAAGAAGATGGAGGGT	TCAGCAGGTAATGTTCGGGCAAT
Human ALKBH5	AGTTCAAGCCTATTCGGGTGTCG	GATCTGAAGCATAGCTGGGTGGTAA
Human WTAP	CTCCCTCAGCGCCATTTTGT	ACAAAATGGCGCTGAGGGAG
Human GAPDH	GAATGGGCAGCCGTTAGGAAAGC	AGCATCACCCGGAGGAGAAATCG
Mouse Il1b	CAAGCAATACCCAAAGAAGAAGA	ATTAGAAACAGTCCAGCCCATAC
Mouse Il6	GGAGCCCACCAAGAACGATAGTCAA	GTCACCAGCATCAGTCCCAAGAA

Mouse Il8	GGCTTTGCGTTGATTCTGGGAACT	AGCGGTGTCCTGATTATCGTCCT
Mouse Il13	GATTCCCTGACCAACATCTCCAA	ATCTCCCTTCCTCCTCAACCCTC
Mouse Mmp3	TTTGATGCAGTCAGCACCCTCCG	TCGTGCCCTCGTATAGCCCAGAA
Mouse Mmp13	TCACCTGATTCTTGCGTGCTATG	CTTTATCTGTGCTCATCTGTGGC
Mouse Cdkn2a	GCTTCCTGGACACGCTGGTGGTGCT	AAGGCGGGCTGAGGCCGGATTTAG
Mouse Cdkn1a	TGAATACCGTGGGTGTCAAAGCA	AGACAGGGAGGGAGCCACAATAC
Mouse Gapdh	AGGTCGGTGTGAACGGATTTG	TGTAGACCATGTAGTTGAGGTCA

Table S6. Primers used for m^{6}A MeRIP-qPCR analysis.

		Primer sequence (5'-3')	
Gene	Sites	Forward	Reverse
ATG7	Site 1	GGAGGCAAGAAATAATGGCG	AAGGCACTACTAAAAGGGGCAA
ATG7	Site 2	ACCCAGAAGAAGCTGAACGAGT	CCCAGCAGAGTCACCATTGTAG
ATG7	Site 3	CGGACCTTGGACCAGCAG	ACAGATACCATCAATTCCACGG
ATG7	Site 4	TGAGGAGCTCTCCATCGCC	GACCTCGGGGTATGGAGGAG
ATG7	Site 5	CTTGGCCTTGCTATTGACCTG	TGGGGGATGGCTATCAGTCA
ATG7	Site 6	TTGGTCCTCCATGCAGTTTTTA	TCAGGGCCAAGGGGAAAG
ATG7	Site 7	AGCTGGGTACGAGACTAAAGGG	AAAGCCATGTCTGAGCAGCTC
ATG7	Site 8	AGTAAAGTGAATATCAAATACCAA	TTATTTTTGTCAGTTACAGTCCTA

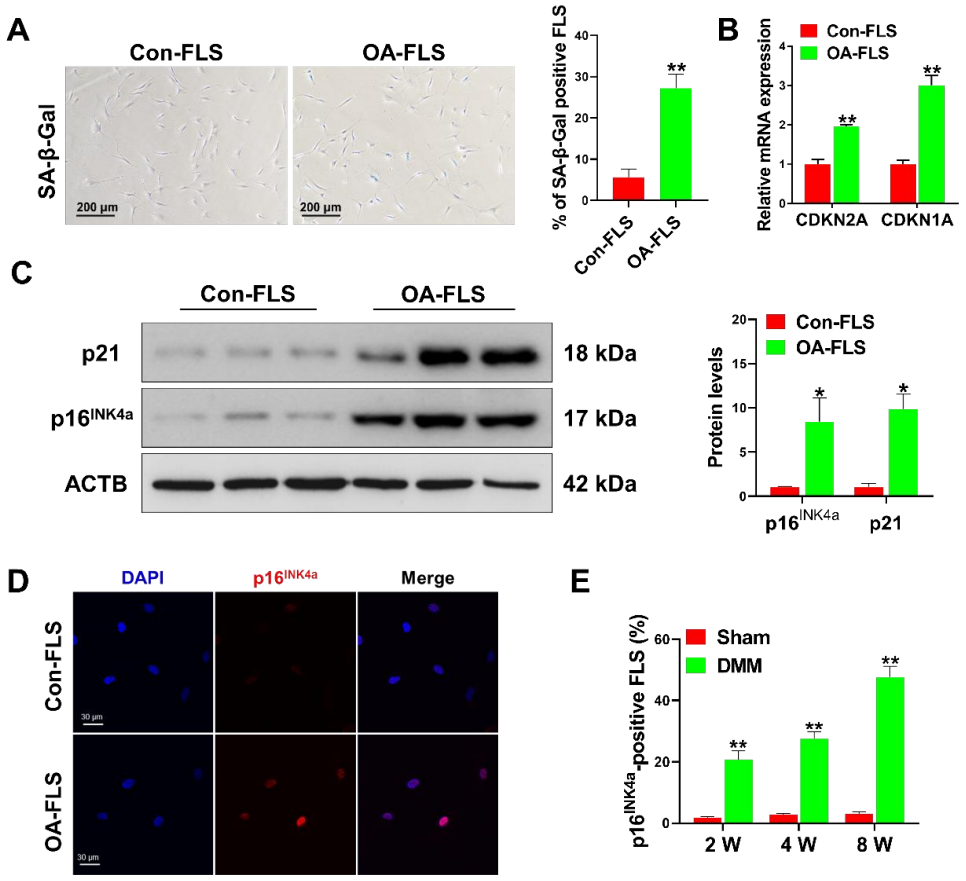

Figure S1. FLS were senescent in the synovium from patients with OA and OA mice. (**A**) The representative images of SA-β-Gal staining FLS (passage 1) derived from synovial tissues of OA patients (OA-FLS) and non-OA patients (Con-FLS) and subsequent quantification of SA-β-Gal positive-staining FLS. n = 3, $^{**}P < 0.01$. (**B**) Q-PCR analysis of mRNA levels for CDKN2A and CDKN1A in human FLS (passage 1) from OA patients (OA-FLS) and non-OA patients (Con-FLS). n = 3, $^{**}P < 0.01$. (**C**) Western blot analysis of $p16^{INK4a}$ and p21 in human FLS (passage 1) from OA patients (OA-FLS) and non-OA patients (Con-FLS). n = 3, $^{*}P < 0.05$. (**D**) The representative images of immunofluorescence staining for $p16^{INK4a}$ in FLS (passage 1) from human normal (Con-FLS) or OA synovium (OA-FLS). (**E**) Quantification of $p16^{INK4a}$-positive FLS as a proportion of total FLS in the synovium from control mice (Sham) or posttraumatic mice at 2, 4 and 8 weeks after destabilisation of the medial meniscus

(DMM) surgery. n = 4 of each group. $^{**}P < 0.01$. All data were presented as the means ± SEM. Paired t test (**A, B, C**) and repeated-measures Two-way ANOVA (**E**) were used for statistical analysis.

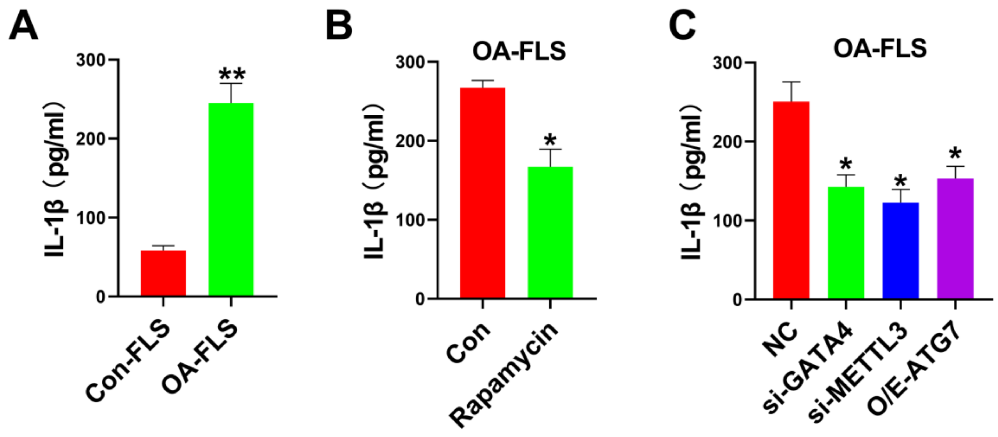

Figure S2. The production of IL-1β in FLS or OA-FLS with various treatment. (**A**) IL-1β levels in the supernatant of FLS or OA-FLS (passage 2). (**B**) IL-1β levels in the supernatant of OA-FLS (passage 2) with or without the treatment of rapamycin. (**C**) IL-1β levels in the supernatant of OA-FLS (passage 2) transfected with siRNA targeting GATA4 (si-GATA4), siRNA targeting METTL3 (si-METTL3) or pcDNA3.1-ATG7 vector (O/E-ATG7). n = 3 of each group. $^{*}P < 0.05$, $^{**}P < 0.01$. All data were presented as the means ± SEM. Paired t test (**A, B**) and one-way ANOVA with Dunnett's multiple comparisons test (**C**) were used for statistical analysis.

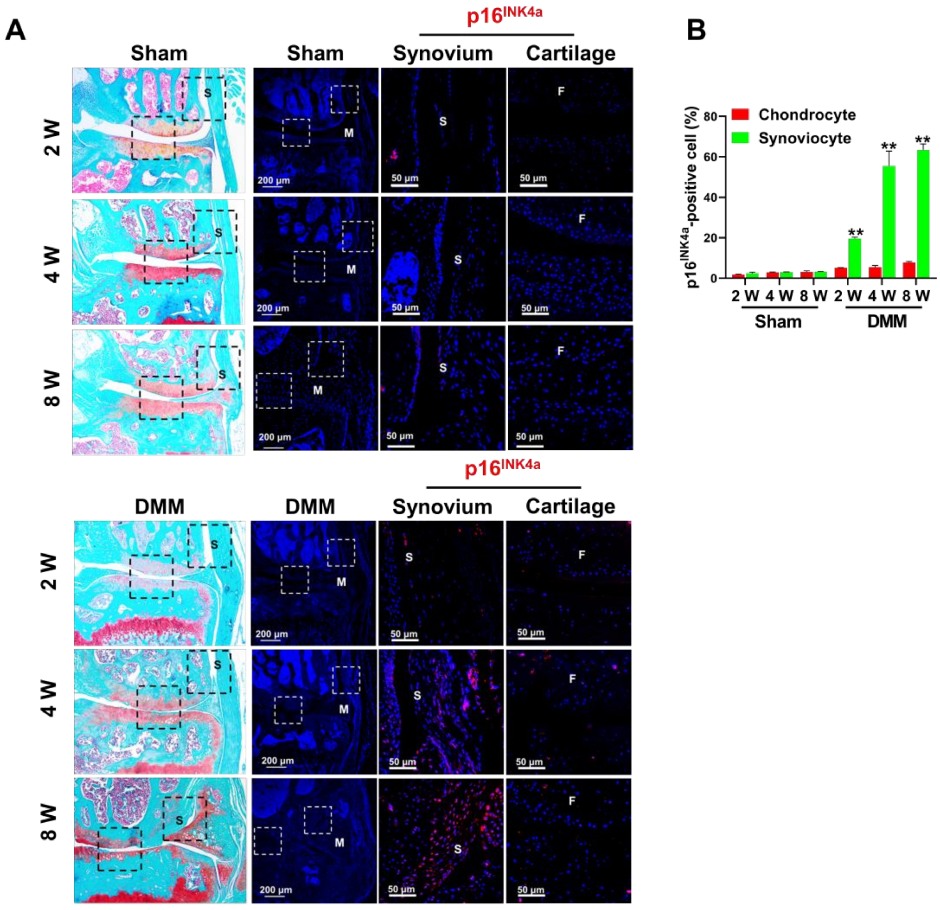

Figure S3. Cellular senescence in the joint of posttraumatic mice at 2, 4 and 8 weeks after DMM surgery. (**A**) Representative images of Safranin O staining and immunostaining for $p16^{INK4a}$ in the cartilage and synovium region from control mice (Sham) or posttraumatic mice at 2, 4 and 8 weeks after destabilisation of the medial meniscus (DMM) surgery. The dotted box indicated the amplified synovium or cartilage regions. (**B**) Quantification of $p16^{INK4a}$-positive FLS as a proportion of total FLS in the synovium from control mice (Sham) or posttraumatic mice at 2, 4 and 8 weeks after destabilisation of the medial meniscus (DMM) surgery. n = 4 of each group. $^{**}P < 0.01$. All data were presented as the means ± SEM. Repeated-measures Two-way ANOVA was used for statistical analysis. F, femur; S, synovium; M, meniscus.

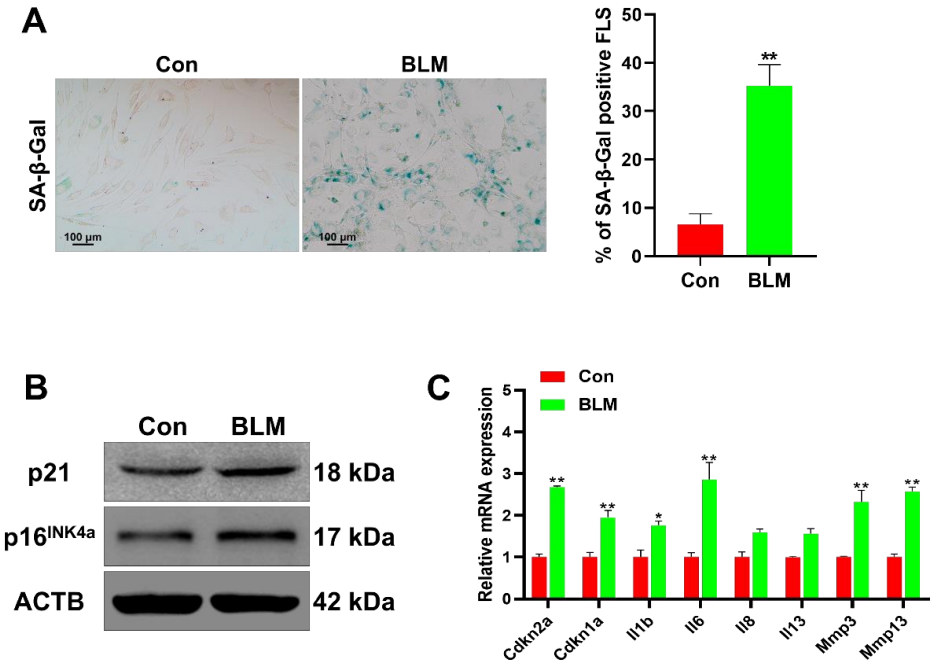

Figure S4. Bleomycin (BLM) induces FLS senescence. (A) The SA-β-Gal staining and semi-quantification of SA-β-Gal level in FLS (Passage 2) isolated from mouse synovium after 7 days of bleomycin (10 μM; n = 5) treatment. $^{**}P < 0.01$. (B) Western blot analysis of $p16^{INK4a}$ and p21 protein levels in mouse FLS (Passage 2) 7 days after treatment with or without BLM. (C) Q-PCR analysis for the mRNA expression of Cdkn2a, Cdkn1a, Il1b, Il6, Il8, Il13, Mmp3 and Mmp13 in mouse FLS with or without the treatment of BLM. n = 3, $^{*}P < 0.05$, $^{**}P < 0.01$. All data were presented as the means ± SEM. Paired t test was used for statistical analysis.

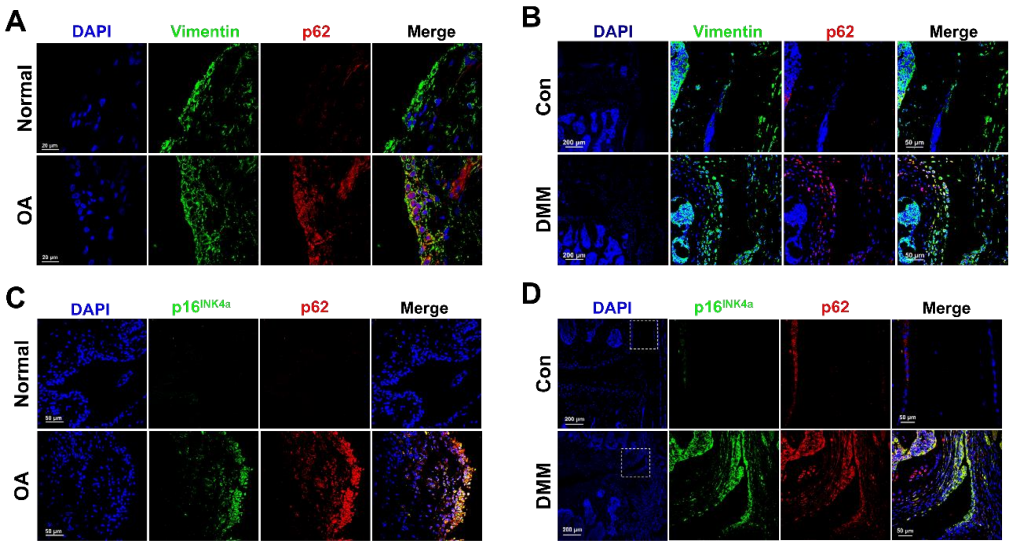

Figure S5. Autophagy is impaired in FLS from patients with OA and DMM-induced OA mice. (**A, B**) The representative images of co-immunostaining of Vimentin and p62 in the synovium from patients with OA and posttraumatic mice 8 weeks after destabilisation of the medial meniscus (DMM) surgery. (**C, D**) The representative images of co-immunostaining of $p16^{INK4a}$ and p62 in the synovium from patients with OA and posttraumatic mice 8 weeks after DMM surgery. The dotted box indicated the amplified synovium regions.

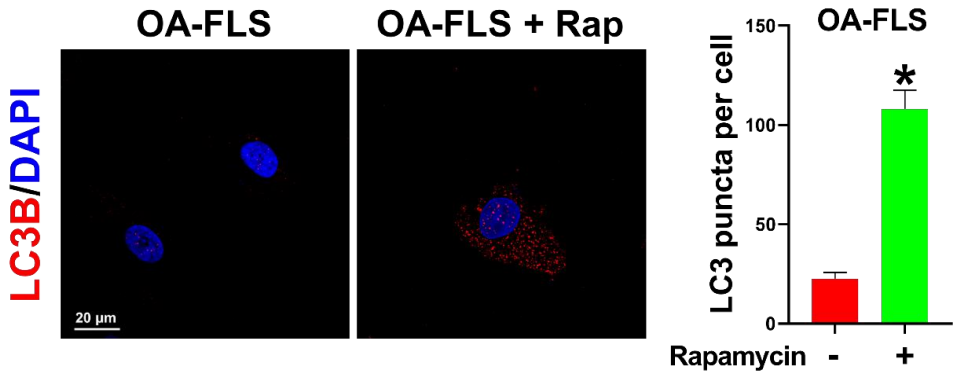

Figure S6. The expression of LC3B in OA-FLS treated with rapamycin. The representative image of immunofluorescent staining of LC3B in human OA-FLS (passage 2) with the treatment of rapamycin or not, and the average number of LC3B

puncta per cell was quantified via imageJ. n = 3 per group, **P* < 0.05. All data were presented as the means ± SEM. Paired t test was used for statistical analysis.

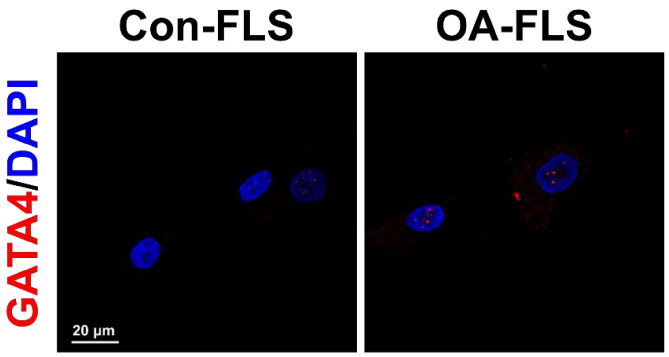

Figure S7. The expression of GATA4 in human FLS from OA patients. The representative images of immunofluorescent staining of GATA4 in human Con-FLS and OA-FLS (passage 2).

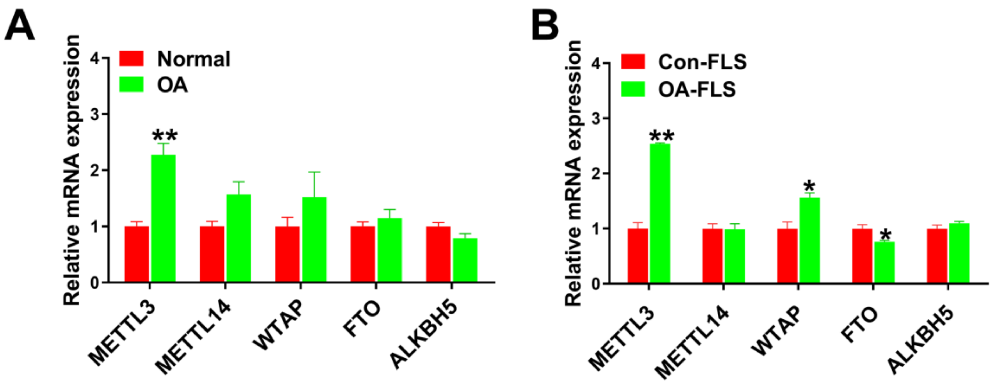

Figure S8. The expression of m^{6}A regulatory enzymess *in vivo* and *in vitro*. (**A, B**) Q-PCR analysis of mRNA levels for METTL3, METTL14, WTAP, FTO and ALKBH5 in human synovial tissues (**A, n = 10**) and FLS (passage 2) derived from OA patients or non-OA patients (**B, n = 3**). **P* < 0.05, ***P* < 0.01. All data were presented as the means ± SEM. Paired t test was used for statistical analysis.

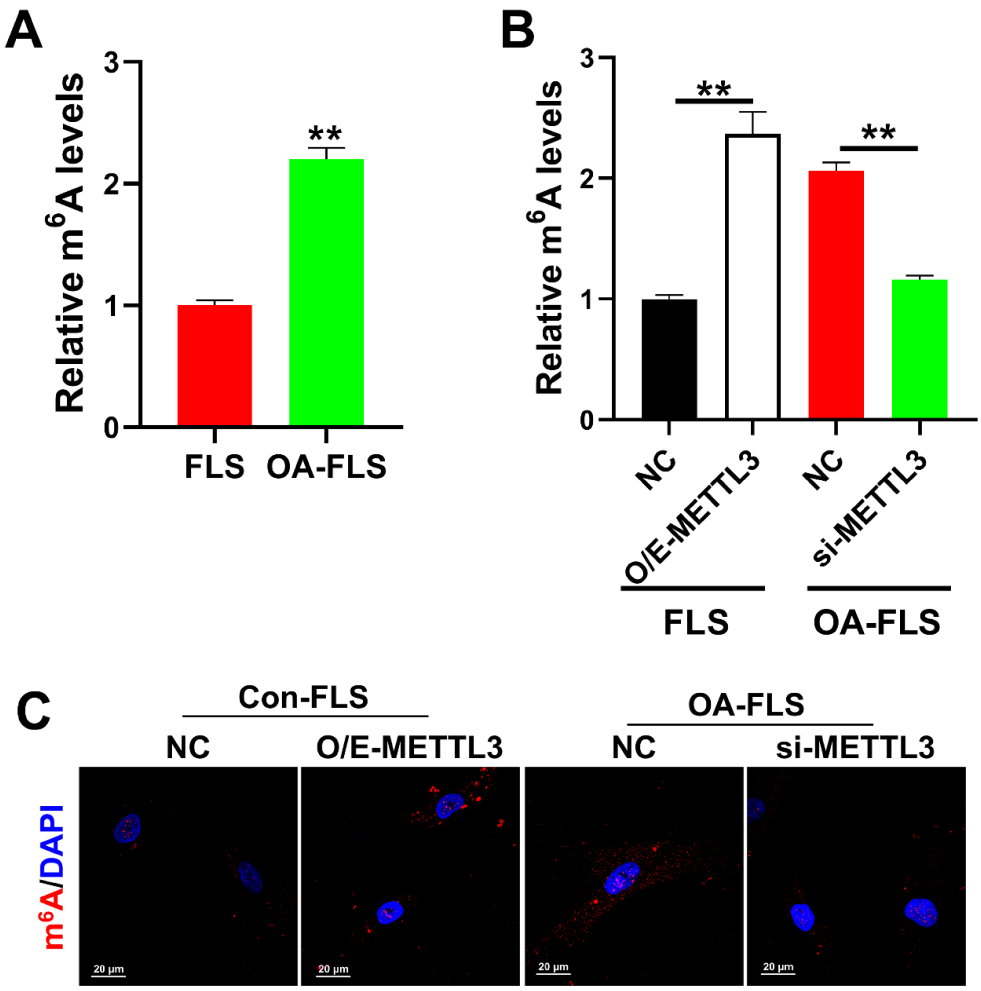

Figure S9. METTL3 regulates m^{6}A levels in human FLS. (**A**) Relative m^{6}A levels were measured by ELISA-based m^{6}A quantitative analyses in human FLS and OA-FLS. n = 3 per group, $^{**}P < 0.01$. (**B**) FLS (passage 2) were transfected with pcDNA3.1-METTL3 vector (O/E-METTL3; O/E, overexpression), and OA-FLS were transfected with siRNA targeting METTL3 (si-METTL3). Relative m^{6}A levels were measured by ELISA-based m^{6}A quantitative analyses. n = 3 per group, $^{**}P < 0.01$. (**C**) The representative images of immunofluorescent detection of m^{6}A in human Con-FLS and OA-FLS (passage 2) treated as in B. All data were presented as the means ± SEM. Paired t test (**A**) and one-way ANOVA with Dunnett's multiple comparisons

test (**B**) were used for statistical analysis.

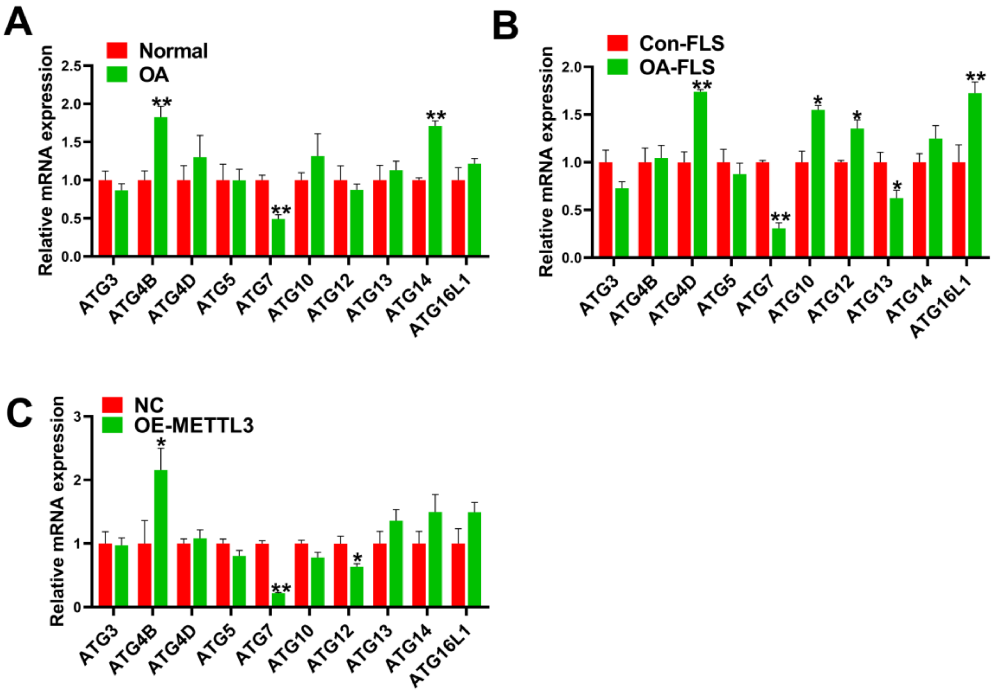

Figure S10. The expression of ATGs in vivo and in vitro. (**A, B**) Q-PCR analysis of mRNA levels for autophagy-related ATGs (ATG6, ATG4B, ATG4D, ATG6, ATG7, ATG10, ATG12, ATG13, ATG14 and ATG16L1) in synovial tissues (**A**) and FLS (**B**) derived from OA patients or non-OA patients. (**C**) Q-PCR analysis of ATGs mRNA expression in human Con-FLS transfected with or without pcDNA3.1-METTL3 vector (O/E-METTL3; O/E, overexpression). All data were presented as the means ± SEM. Paired t test was used for statistical analysis. *$P < 0.05$, **$P < 0.01$.

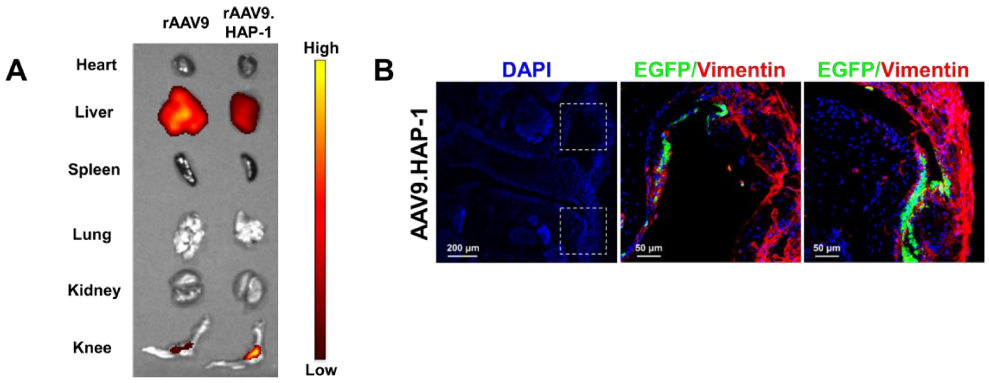

Figure S11. The FLS specificity of rAAV9.HAP-1. (**A**) The fluorescence signal of EGFP in individual organs and tissues (heart, liver, spleen, lung, kidney and keen joint) from mice after intra-articular injection with a signal dose of 2×10^{11} genome copies of rAAV9 or rAAV9.HAP-1. (**B**) Confocal microscope analysis of co-staining of Vimentin and EGFP in the knee joints from mice after intra-articular injection with rAAV9 or rAAV9.HAP-1.

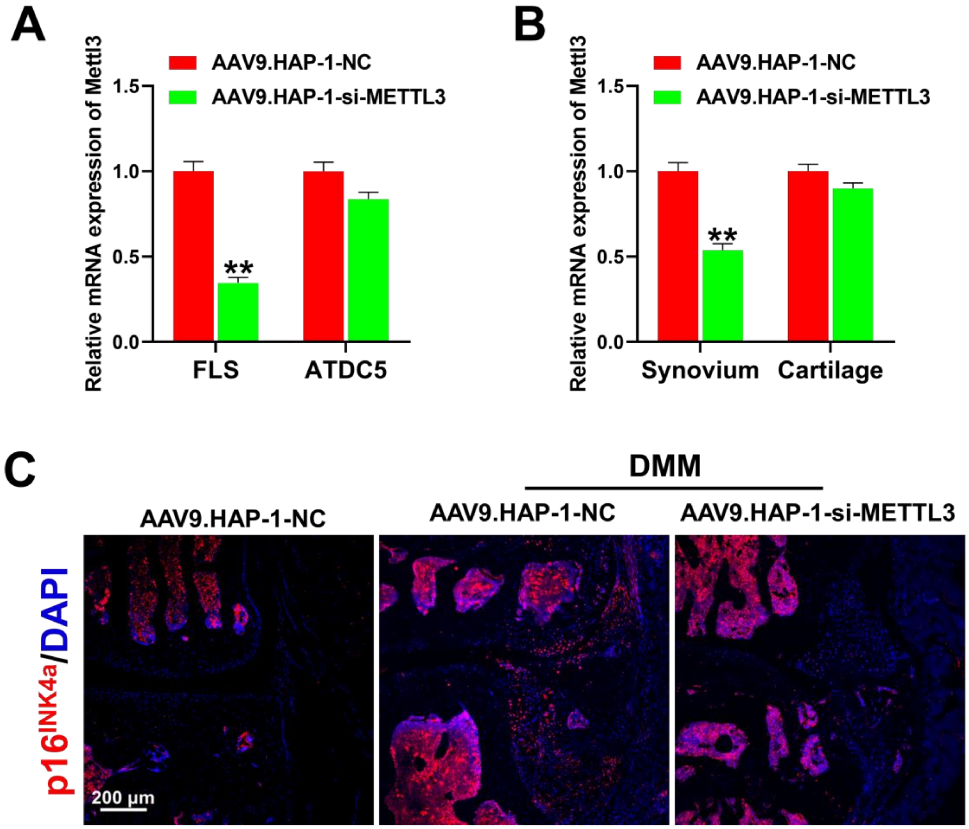

Figure S12. Targeted inhibition of METTL3 in FLS suppresses the expression p16^{INK4a} in vivo. (A) Q-PCR analysis of mRNA levels for METTL3 in FLS (passage 2) and ATDC5 cells transfected with rAAV9.HAP-1-NC or rAAV9.HAP-1-si-METTL3. n = 3, $^{**}P < 0.01$. (B) Q-PCR analysis of mRNA levels for METTL3 in the cartilage and synovium of mice treated with rAAV9.HAP-1-NC or rAAV9.HAP-1-si-METTL3. n = 3, $^{**}P < 0.01$. (**C**) The representative images of immunofluorescent staining of p16^{INK4a} in the knee joint from DMM-induced OA mice after intra-articular injection with rAAV9.HAP-1-NC and rAAV9.HAP-1-si-METTL3. All data were presented as the means ± SEM. Paired t test was used for statistical analysis.